

## Factors affecting distribution of dose in horizontal direction during irradiation

Chang-Ho Cho<sup>1</sup>, Jeong-Lae Kim<sup>2\*</sup>, GeonUk Kang<sup>3</sup>

<sup>1,2</sup>Department of Biomedical Engineering, Eulji University, Seongnam, 13135, Korea; jlkim@eulji.ac.kr (J.L.K.)

<sup>3</sup>Department of Applied Smart Factory, SungKyunKwan University, Suwon, 16419, Korea.

**Abstract:** Recording and managing the dose of x-rays in an x-ray machine is an important part of the data. In addition, recording and managing radiation dose data in x-ray devices plays an important role in providing transparency of radiation dose to medical staff and patients by quantifying the radiation dose data. Four mobile diagnostic X-ray units were used to analyze the dose by spatial location. The dose distribution by location was analyzed by identifying and analyzing the dose by angle for both image intensifier and flat panel detector types. The three-dimensional space of the radiation area consisted of 27 sides, and the structure of the space was assumed to be horizontal X, Y, and Z sides and vertical A, B, and C sides, and the dose analysis was performed at the assumed position. On the longitudinal side, the highest dose tissue (highest  $\mu\text{Sv}/\text{min}$ ) is B\_Center : (R.B.M, Colon, Lung, Stomach, Breasts, Remainder of body) - 330.404  $\mu\text{Sv}/\text{min}$ , and the lowest dose tissue (lowest  $\mu\text{Sv}/\text{min}$ ) is 0.002  $\mu\text{Sv}/\text{min}$  on the (Skin, Bone surface, Salivary glands, Brain) side at C\_270°. The findings from diagnostic X-ray devices have emphasized the importance of managing radiation exposure when using the devices and may raise questions about the management of radiation protection measures to protect the health of healthcare personnel and patients. This can be expected to advance the organization of the use of radiation devices in a safe healthcare environment. A system for managing data will be useful as an indicator to guide medical staff using the equipment and patients participating in procedures and surgeries where they can minimize their dose and avoid harm.

**Keywords:** Diagnostic radiology equipment, Radiation exposure dose, C-arm, Shielding material, Dose information.

### 1. Introduction

Radiation protection is a requirement when using radiation, and radiation dose measurement plays an important role. As medical and research advances in radiation protection, there is a need for technologies that can produce radiation fields of high intensity, very short duration, and high repetition rate [1]. These new technologies include accelerators and ultra-high-intensity laser devices that produce high-intensity neutron sources at intermediate energies from about 50 MeV to several GeV per nucleon [2,3]. For example, at J-PARC's 1 MW proton accelerator, the maximum extraction energy, current, and number of neutrons produced at 3 GeV (333 mA) each provide an average neutron yield of  $3 \times 10^{18} \text{ s}^{-1}$  [4]. Ultra-intense lasers interact with a target with powers ranging from a few hundred TW to a few PW, accelerating a large number of electrons down to tens of MeV, which generate a very strong electric field of the order of a few TV  $\text{m}^{-1}$  that ionizes the backside of the target [5]. The electric field generated here can accelerate the ions to tens of MeV and creates the characteristic of Bremsstrahlung, which interacts with the chamber using X-rays [6].

Secondary neutrons can also be present when the energy from photons and ions exceeds the threshold for production. The duration of a single laser pulse is in the order of a few hundred fs, so that measurements are made on the primary ions of the target and the secondary radiation field, neutrons.

The detectors used for radiation protection are TLDs for photons and passive detectors in superheated emulsions for neutrons [7]. The application of ionizing radiation to medical imaging is intended to be used in medical practice to improve human health [8]. The effects of radiation exposure on the human body are generally increased and the consequences of this increase in radiation dose require a higher level of radiation protection for the patient [9]. In many healthcare settings, occupational radiation doses to users and healthcare personnel are monitored [10] and direct dose data are required for outcomes [11]. The utilization of medical imaging has been increasing in recent decades, with a significant increase in the total volume of radiological imaging [12]. The radiation protection of patients with increased radiation exposure requires increased utilization and a higher level of care [13]. The risk of low-dose radiation in medical imaging is unproven, and it is difficult to demonstrate a risk for low-dose radiation [14,15].

In order to establish dose information based on the location of low-dose sources with risk implications [16], specific measures of dose in the dose monitoring system are required. Exposure management is based on the structural location of low doses and converting them into dose measurements, so we want to find a way to calculate the ionizing radiation from the measuring device. Through, the measurement value of ionizing radiation is materialized and utilized for statistical data of radiation dose.

## 2. Methods

### 2.1. Instruments

A dose monitoring system should be established to locate low doses of potentially hazardous sources. Dosimetry requires a radiation-protected detector to measure low doses and uses a passive detector with a TLD for photons and a superheated emulsion for neutrons. A typical detector is the Radical 9010 10X5-1800 Ion Chamber Table 1.

**Table 1.**  
Ion chamber specifications.

Chamber	Radical 9010 10X5-1800 ion chamber	
Minimum rate	0.01 mR/hr	0.1 µGy/hr
Maximum rate	65 R/hr	575 mGy/hr
Minimum dose	0.1 µR	0.01 nGy
Maximum dose	230 R	2 Gy
Cine specifications	N/A	
Calibration accuracy	±4% using X-rays @ 150 kVp & 10.2mm Al HVL	
Exposure rate dependance	+0%, -5%, 0.1mR/hr to 20 R/hr, -10% to 65 R/hr	
Energy dependance	±5%, 33 keV to 1.33 MeV (with build-up material)	
Construction	Polycarbonate walls and electrode;	
	conducting graphite exterior coating; 1800cm <sup>3</sup> active volume; 0.54 kg	

### 2.2. Diagnostic Radiation Device for Measurement Equipment

We found a method to construct low-dose radiation structurally according to positional changes, measure the dose by ionization changes, and calculate the converted value from the measurement device. The equipment used for measurement is FPD (Flat Panel Detector) and I.I (Image Intensifier). The types of X-ray devices are Korean FPD C-arm, German FPD C-arm, Korean Image Intensifier C-arm, and German Image Intensifier C-arm, which have different characteristics of C-arm. In order to evaluate the reliability of the dose, the average dose value calculated from the German Image Intensifier C-arm was used as a reference value.

### 2.3. Experimental Method

- Dose Measurement Procedure According to Position

1. Divide the space into 27 sections, centered on the center of the X, Y, and Z planes, by creating 9 sections at  $45^\circ$  intervals and further categorizing them into three sides : A, B, and C.

2. Set the measurement voltage to 50-110 kV (in 10 kV increments) and the current to 1-4 mA (in 1 mA increments), then measure the irradiation dose in the 27 sections.

3. Analyze the measured dose values for reliability using variance analysis.

4. Convert the measured irradiation dose to absorbed dose. Irradiation dose (X) refers to the amount of ionizing radiation measured in air, typically in units of Roentgen (R). Absorbed dose (D) refers to the amount of radiation absorbed by a specific substance (e.g., human tissue), typically in units of Gray (Gy). The absorbed dose can be calculated from the irradiation dose using the air kerma rate ( $f$ ), where  $f$  is a conversion factor specific to the material.

$$D = X \cdot f \quad (1)$$

5. Since the effect of radiation on tissue varies depending on the type and energy of the radiation, the equivalent dose (H) is calculated by taking this into account. The equivalent dose is calculated by multiplying the absorbed dose by the radiation weighting factor ( $W_R$ ).

$$H = D \cdot W_R \quad (2)$$

$W_R$  is a value determined by the type of radiation (e.g., X-rays, gamma rays, and electromagnetic waves have a value of 1; neutrons, depending on their energy, have a value of 2.5-20; protons have a value of 2; and alpha particles have a value of 20).

6. When converting from equivalent dose to effective dose, the effective dose (E) is a value that takes into account the sensitivity of various organs or tissues to radiation. The effective dose is calculated by multiplying the equivalent dose of each organ or tissue by the tissue weighting factor ( $W_T$ ).

$$E = \sum_T (H_T \cdot W_T) \quad (3)$$

$W_T$  is a factor that represents the radiation sensitivity of a specific organ or tissue.

7. The coefficients required in this process ( $f$ ,  $W_R$ ,  $W_T$ ) should use the standard values provided by organizations such as the International Commission on Radiological Protection (ICRP).

For example, to calculate the dose based on the measured values: If the irradiation dose X is 1 R (Roentgen), the absorbed dose D is calculated as follows.

$$D = X \cdot f \times 0.00876 \text{ Gy} / \text{R} = 0.00876 \text{ Gy} \quad (4)$$

Here, 0.00876 Gy/R is the typical value for the air kerma rate. If the absorbed dose D is 0.00876 Gy, and if the radiation is X-rays, the equivalent dose H is calculated as follows.

$$H = D \cdot W_R = 0.00876 \text{ Gy} \times 1 = 0.00876 \text{ Sv} \quad (5)$$

If the equivalent dose H is 0.00876 Sv, the effective dose E is calculated as follows (considering the contribution of each tissue):

$$E = \sum_T (H_T \cdot W_T) \quad (6)$$

For example, if the exposed organ is the lungs:

$$E_{\text{lung}} = H_{\text{lung}} \cdot W_{\text{lung}} = 0.00876 \text{ Sv} \times 0.12 = 0.0010512 \text{ Sv} \quad (7)$$

By summing up the contributions from each organ in this manner, the total effective dose E can be obtained. The example above serves as a simple illustration for clarity. In actual calculations, all exposed organs and tissues must be considered.

### 3. Research Results

#### 3.1. Validation of Radiation Dose From C-Arm Equipment

The average differences in radiation dose among four C-arm diagnostic radiation devices were verified. After validating 756 absorbed dose values for each device, the p-value was found to be less than .001, indicating that the differences in radiation dose among each device were statistically significant, with values less than .05 confirming the presence of differences in radiation dose between each device

(Table 2).

**Table 2.**

Validate average differences in radiation dose across devices.

Classification by equipment	Mean	Std. deviation	F	Sig. (P)
Korean flat panel type C-arm	39929.03	174702.866	5.534	.001
Korean image intensifier type C-arm	16886.87	75645.082		
German flat panel type C-arm	19307.08	89619.372		
German image intensifier type C-arm	24478.61	119369.526		

### 3.2. Verification of Radiation Dose According To A, B, C Planes

The average differences according to the A, B, and C planes were verified. The p-value was found to be less than .001, indicating that the differences in radiation dose among each side were statistically significant with values less than .05. Post-hoc tests were conducted to specifically verify the mean differences between groups. Analysis revealed that radiation dose in B (M=74777.19, SD=201050.348) was significantly higher compared to A (M=394.369, SD=480.411) and C (M=279.639, SD=538.719) Table 3.

**Table 3.**

Verification of mean differences in radiation dose by side.

	N	Mean	Std. deviation	F	Sig.	POST_HOC
A	1008	394.37	480.411	138.185	0.000	B>A, C
B	1008	74777.19	201050.348			
C	1008	279.64	538.719			

### 3.3. Analysis of X-Axis (A, B, C\_45°, 90°, 135°) Dose Areas

1. R.B.M, Colon, Lung, Stomach, Breasts, Remainder of body show maximum dose at B\_90°, with 139.855  $\mu\text{Sv}/\text{min}$  for each tissue. They show minimum dose at C\_90°, with 0.054  $\mu\text{Sv}/\text{min}$  for each tissue.

2. Gonads show maximum dose at B\_90°, with 93.237  $\mu\text{Sv}/\text{min}$ . They show minimum dose at C\_90°, with 0.036  $\mu\text{Sv}/\text{min}$ .

3. Bladder, Liver, Oesophagus, Thyroid show maximum dose at B\_90°, with 46.618  $\mu\text{Sv}/\text{min}$  for each tissue. They show minimum dose at C\_90°, with 0.018  $\mu\text{Sv}/\text{min}$  for each tissue.

4. Skin, Bone surface, Salivary glands, Brain show maximum dose at B\_90°, with 11.655  $\mu\text{Sv}/\text{min}$  for each tissue. They show minimum dose at C\_90°, with 0.004  $\mu\text{Sv}/\text{min}$  for each tissue (Fig. 1).

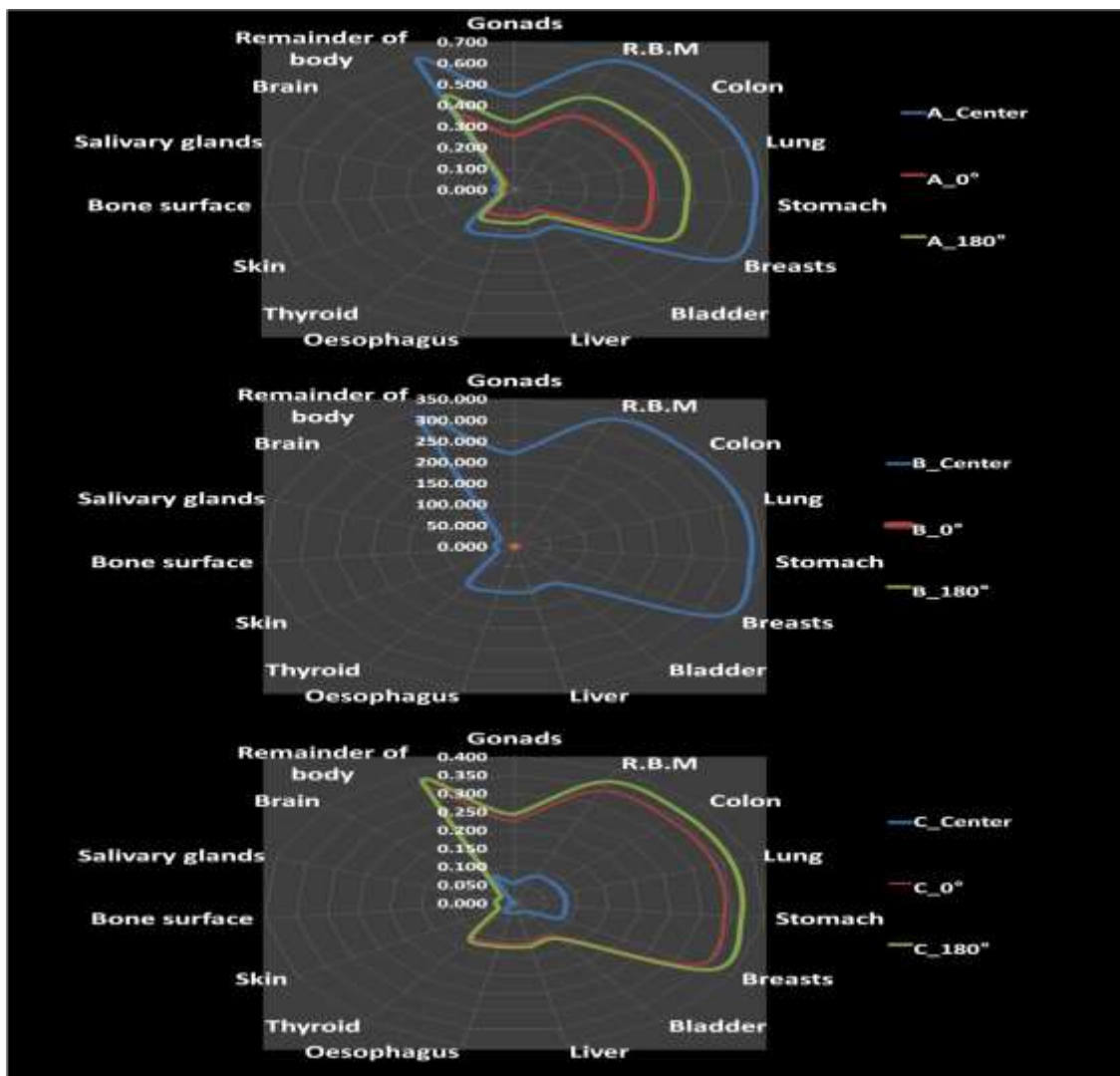


**Figure 1.**  
Radiation Distribution Profiles for A, B, C Sides at Center, 0°, 180°.

#### 3.4. Analysis of Y-Axis (A, B, C\_Center, 0°, 180°) Dose Areas

1. R.B.M, Colon, Lung, Stomach, Breasts, Remainder of body show maximum dose at B\_Center, with 330.404  $\mu\text{Sv}/\text{min}$  for each tissue. They show minimum dose at C\_Center, with 0.082  $\mu\text{Sv}/\text{min}$  for each tissue.

2. Gonads show maximum dose at B\_Center, with 220.269  $\mu\text{Sv}/\text{min}$ . They show minimum dose at C\_Center, with 0.055  $\mu\text{Sv}/\text{min}$ .

3. Bladder, Liver, Oesophagus, Thyroid show maximum dose at B\_Center, with 110.135  $\mu\text{Sv}/\text{min}$  for each tissue. They show minimum dose at C\_Center, with 0.027  $\mu\text{Sv}/\text{min}$  for each tissue.

4. Skin, Bone surface, Salivary glands, Brain show maximum dose at B\_Center, with 27.534  $\mu\text{Sv}/\text{min}$  for each tissue. They show minimum dose at C\_Center, with 0.007  $\mu\text{Sv}/\text{min}$  for each tissue (Fig. 2).

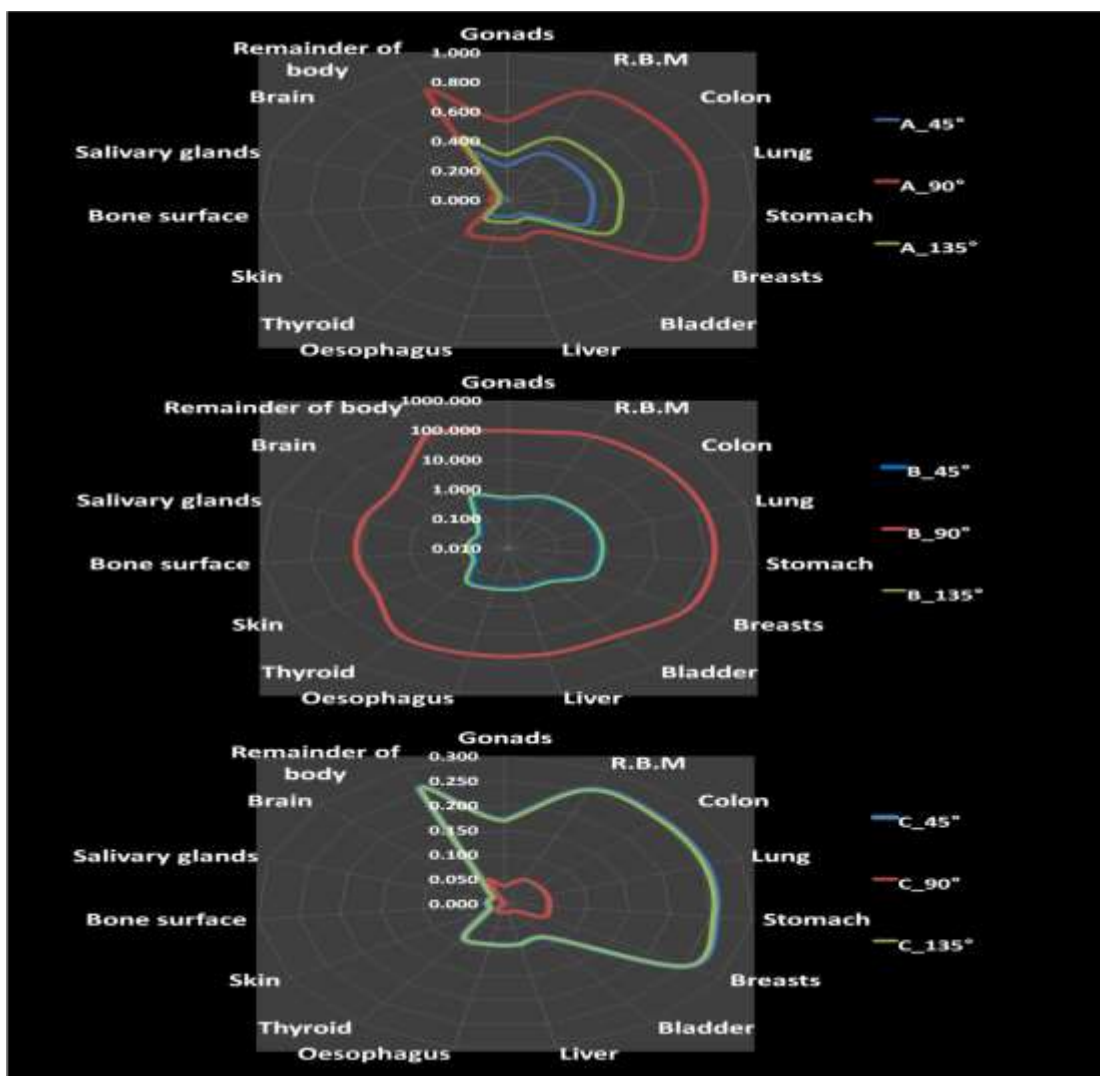


**Figure 2.**  
Radiation Distribution Profiles for A, B, C Sides at 45°, 90°, 135°.

### 3.5. Analysis of Z-Axis (A, B, C\_225°, 270°, 315°) Dose Areas

1. R.B.M, Colon, Lung, Stomach, Breasts, Remainder of body showed maximum dose at C\_315°, with 0.269  $\mu\text{Sv}/\text{min}$  for each tissue. They showed minimum dose at C\_270°, with 0.019  $\mu\text{Sv}/\text{min}$  for each tissue.

2. Gonads showed maximum dose at C\_315°, with 0.180  $\mu\text{Sv}/\text{min}$ . They showed minimum dose at C\_270°, with 0.013  $\mu\text{Sv}/\text{min}$ .

3. Bladder, Liver, Oesophagus, Thyroid showed maximum dose at C\_315°, with 0.090  $\mu\text{Sv}/\text{min}$  for each tissue. They showed minimum dose at C\_270°, with 0.006  $\mu\text{Sv}/\text{min}$  for each tissue.

4. Skin, Bone surface, Salivary glands, Brain showed maximum dose at C\_315°, with 0.022  $\mu\text{Sv}/\text{min}$  for each tissue. They showed minimum dose at C\_270°, with 0.002  $\mu\text{Sv}/\text{min}$  for each tissue (Fig. 3).

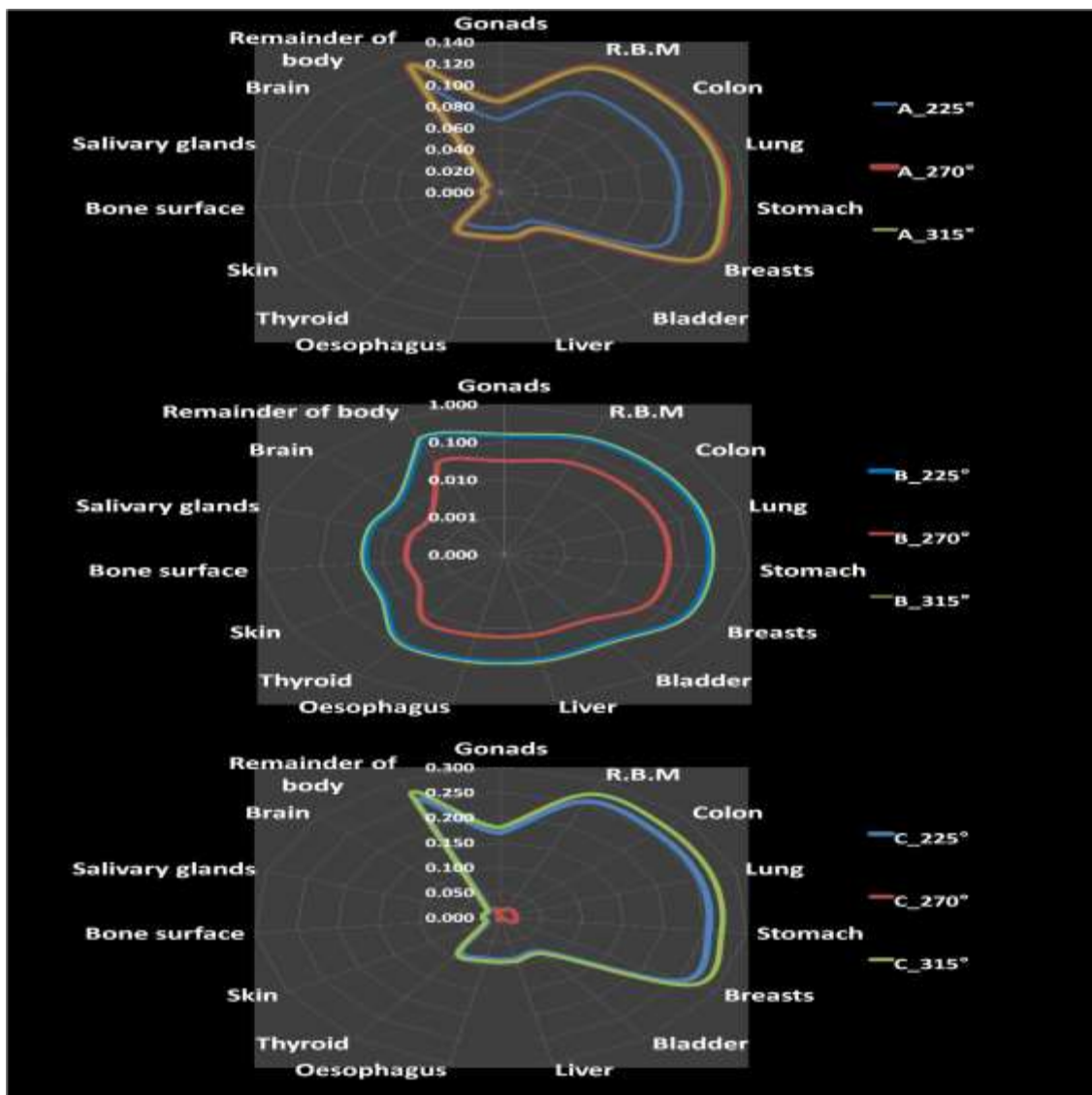


**Figure 3.**  
Radiation Distribution Profiles for A, B, C Sides at 225°, 270°, 315°.

#### 4. Discussion

Analyzing the radiation exposure levels of C-arm equipment used in medical imaging, we focused on investigating the differences in radiation dose among A, B, and C sides. From this analysis, the following conclusions were drawn: Significant differences in radiation dose were observed among the four types of C-arm equipment. The German Image Intensifier type C-arm showed higher radiation levels compared to other devices. Radiation dose on the B side was notably higher than on the A and C sides. High radiation exposure at specific locations indicates the necessity for radiation protection measures. Radiation levels varied significantly along the X, Y, and Z axes based on direction and position. Most tissues exhibited maximum radiation exposure at B<sub>90°</sub> and minimum at C<sub>90°</sub>. Specific management and supervision are required to minimize radiation exposure. Measures such as using radiation protection equipment and reducing exposure time are necessary when working in high-exposure areas like the B side. Further research is needed to investigate radiation levels in diverse medical environments and study the long-term effects of radiation exposure. Strengthening radiation

protection education is essential to minimize radiation exposure among medical staff.

## 5. Conclusion

In order to establish dose information according to the location of low doses, a dose monitoring system is established and organized for accurate diagnosis and examination according to the dose measurement method. Since the increase in radiation dose caused by using radiation is a situation where the use of imaging is increasing to obtain better image quality in medical information, the increased radiation dose is used for the patient's exposure level and managed to monitor the radiation dose of users and medical staff. The devices used were four mobile diagnostic X-ray units, and the doses were analyzed by spatial location. To understand the dose distribution by location, angular dose was analyzed for image intensifier and flat panel detector types. Depending on the scope of the section used, the three-dimensional space of the radiation source was constructed with 27 sides, and the structure of the space was assumed to be the horizontal X, Y, and Z sides and the vertical A, B, and C sides. In order to build the dose information according to the location of the low dose, the dose measurement method was made possible by the dose monitoring system. In the exposure control, the method of converting the ionizing radiation from the measuring device to the measured value of the dose due to the structural position change of the low dose was utilized. This allows the measurement of ionizing radiation to be materialized, which can be used as a step for statistical data on radiation dose in the future.

## Copyright:

© 2024 by the authors. This article is an open access article distributed under the terms and conditions of the Creative Commons Attribution (CC BY) license (<https://creativecommons.org/licenses/by/4.0/>).

## References

- [1] Schwoerer, H., Pfothner, S., Jäckel, O., Amthor, K.-U., Liesfeld, B., Ziegler, W., Sauerbrey, R., Ledingham, K.W.D., Esirkepov, T., Laser-plasma acceleration of quasi-monoenergetic protons from microstructured targets. *Nature* 439 (26), 445e448 (2006).
- [2] Wyatt, R.W.W., Wyborn, B.E., Radiological characterisation of photon radiation from ultra-high-intensity laser-plasma and nuclear interactions. *J. Radiol. Prot.* 26, 277e286 (2006).
- [3] Wagner, R., Bräutigam, W., Filges, D., Ullmaier, H., 2000. The project "European Spallation Source (ESS)": status of R&D programme. *Physica B*, 38e44. Wei, J., 2002. The spallation neutron source project. Proceedings of the Eight European Particle Accelerator Conference EPAC 2002, Paris, France, 3e7 (June 2002), ISSN 1684-761X (Web version) 1064e1066.
- [4] Borne, F., Delacroix, D., Gelé, J.M., Massé, D., Amiranoff, F., Radiation protection for an ultra-high intensity laser. *Radiat. Prot. Dosim.* 102, 61e70 (2002).
- [5] Clarke, R.J., Neely, D., Edwards, R.D., Wright, P.N.M., Ledingham, K.W.D., Heathcote, R., McKenna, P., Danson, C.N., Brummitt, P.A., Collier, J.L., Hatton, P.E.,
- [6] Hegelich, B.M., Albright, B.J., Cobble, J., Filippo, K., Letzring, S., Paffett, M., Ruhl, H., Schreiber, J., Scultze, R.K., Fernández, J.C., Laser acceleration of quasihomogeneous MeV ion beams. *Nature* 439 (26), 441e444 (2006).
- [7] Ikeda, S., Japanese spallation neutron source. *Appl. Phys.* 74, S-15eS-17 (2002).
- [8] United nations scientific committee on the effects of atomic, Sources and Effects of Ionizing Radiation, UNSCEAR 2008 Report to the General Assembly with Scientific Annexes, Vol. 1: Sources, United Nations, New York (2010).
- [9] International atomic energy agency, Patient Dose Optimization in Fluoroscopically Guided Interventional Procedures, IAEA-TECDOC-1641, IAEA, Vienna (2010).
- [10] Padovani, R., Le Heron, J., Cruz-Suarez, R., et al., 2011. International project on individual monitoring and radiation exposure levels in interventional cardiology. *Radiat. Prot. Dosim.* 144, 437–441.
- [11] IAEA, 2014b. Recommendations of the Working Group on Interventional Cardiology on Occupational Doses to the Lens of the Eye in Interventional Cardiology: the Information System on Occupational Exposure in Medicine, Industry and Research (ISEMIR). IAEA-TECDOC-1735. International Atomic Energy Agency, Vienna.
- [12] Tsapaki, V., Ahmed, N.A., AlSuwaidi, J.S., et al., 2009. Radiation exposure to patients during interventional procedures in 20 countries: initial IAEA project results. *Am. J. Roentgenol.* 193, 559–569.
- [13] Kim, K.P., Miller, D.L., Balter, S., et al., 2008. Occupational radiation doses to operators performing cardiac catheterization procedures. *Health Phys.* 94, 211–227.
- [14] International atomic energy agency, SSDL Network Charter, The IAEA/WHO Network of Secondary Standards Dosimetry Laboratories, IAEA, Vienna (2018).



- [15] United nations scientific committee on the effects of atomic, Sources, Effects and Risks of Ionizing Radiation, UNSCEAR 2020/2021 Report, Volume 1: Report to the General Assembly, Scientific Annex A: Evaluation of Medical Exposures to Ionizing Radiation, United Nations, New York (2022).
- [16] Linet, Martha S.; Slovis, Thomas L.; Miller, Donald L.; Kleinerman, Ruth; Lee, Choonsik; Rajaraman, Preetha; Berrington de Gonzalez, Amy Cancer risks associated with external radiation from diagnostic imaging procedures, CA: A Cancer Journal for Clinicians. 62 (2): 75–100 (March 2012).